

Rotorcraft model identification: a black-box time/frequency domain approach

Marco Bergamasco¹

Marco Lovera²

¹ Leonardo Helicopter Division (Italy), Aircraft System Integration D&D - Flight Mechanics
marco.bergamasco02@leonardocompany.com

² Dipartimento di Scienze e Tecnologie Aerospaziali, Politecnico di Milano, Italy
marco.lovera@polimi.it

Abstract: In this paper a time/frequency domain approach to rotorcraft model identification is presented and discussed. The approach uses data collected in different identification experiments (corresponding to the application of frequency sweeps, 3211 and doublet input sequences) to estimate both parametric black-box state-space models using a subspace method and non-parametric estimates of the frequency response function. Results obtained in the flight testing campaign for the identification of linear models of a light utility helicopter are presented to illustrate the performance of the approach.

NOMENCLATURE

a	position of Laguerre pole
f, p	future, past horizon lengths in CT-PBSID algorithm
q, p, r	pitch, roll, and yaw angular rate
v	output noise of state space model
w	process noise of state space model
x	state vector of state space model
y	output vector of state space model
N_x, N_y, N_z	longitudinal, lateral, and vertical accelerations in body reference
$\delta_{lon}, \delta_{lat}$	longitudinal and lateral cyclics
$\delta_{col}, \delta_{ped}$	collective and pedal

1. INTRODUCTION AND MOTIVATIONS

The problem of rotorcraft model identification has been studied extensively over the last few decades and many methods and tools to handle it have been developed^[1,2]. In most of the rotorcraft identification literature either frequency-domain methods or time-domain ones are used. Frequency-domain methods assume that identification-oriented flight testing consists in (manual or automatic) frequency sweeps, through which accurate non-parametric estimates of the frequency response functions associated with the flight dynamics of the helicopter can be computed. Time-domain methods, on the other hand, rely on excitation inputs such as, e.g., the 3211 sequence^[3],

which excites a wide frequency band within a short time period. Both approaches have advantages and disadvantages, but surprisingly enough no significant effort has been made so far to combine the two viewpoints to develop a unified approach allowing the refinement of parametric models using information coming from the two domains. Furthermore, most existing methods solve the parameter estimation problem iteratively, and thus call for an initial guess to start the process which may not be easy to define particularly in multivariable problems.

In the system identification literature, on the other hand, multivariable, non-iterative identification of linear models is routinely addressed using the so-called Subspace Model Identification (SMI) methods^[4,5], which have proven extremely successful in dealing with the estimation of state space models for MIMO systems. Even though SMI methods are particularly well suited for rotorcraft problems (the subspace approach can deal in a very natural way with MIMO problems; in addition, SMI algorithms can be implemented with numerically stable and efficient tools from numerical linear algebra; finally, information from separate data sets, such as data collected during different experiments on the system, can be merged in a very simple way into a single state space model), until recently these methods have received limited attention from the rotorcraft community, with the partial exception of some contributions such as^[6,7,8,9] in which however only methods and tools going back 10 to 15 years in the SMI literature (such as the MOESP algorithm of^[10] and the bootstrap-based method for uncertainty analysis of^[11]) have been considered. Therefore, the further potential benefits offered by the latest developments in the field have not been fully ex-

ploited. Among other things, present-day approaches can provide:

- unbiased model estimates from data collected under feedback (see, *e.g.*,^[12,13,14]), as is frequently the case in experiments for rotorcraft identification^[1];
- analytical^[12,15] and numerical^[11,16] methods to compute the variance of the estimates, which can be used in the eventual assessment of model quality;
- continuous-time models from (possibly non-uniformly) sampled input-output data^[17,18], using data transformations based on, *e.g.*, the Laguerre basis^[19].

Preliminary results obtained using continuous-time SMI on data collected in piloted simulations have been presented in^[20], while a detailed case study dealing with the attitude dynamics of a multirotor UAV has been presented in^[21]. Since then, a systematic approach consisting of a multi-step procedure exploiting the best features of a number of existing methods and tools to achieve identified models of improved accuracy has been developed at Leonardo Helicopters and applied to the problem of characterising the flight dynamics of several prototypes at different forward speeds, altitudes and take-off weights. The identified models have been successfully used for the assessment of the Automatic Flight Control System (AFCS) and for the dynamics validation of a nonlinear physical model.

In this paper the proposed time/frequency domain approach to rotorcraft model identification will be presented and discussed and results obtained in the identification of linear models of a flying helicopter prototype in several flight conditions will be presented.

2. PROBLEM STATEMENT AND PRELIMINARIES

Consider the linear, time-invariant continuous-time model

$$\begin{aligned} \dot{x}(t) &= Ax(t) + Bu(t) + w(t), \quad x(0) = x_0 \\ (1) \quad y(t) &= Cx(t) + Du(t) + v(t) \end{aligned}$$

where $x \in \mathbb{R}^n$, $u \in \mathbb{R}^m$ and $y \in \mathbb{R}^p$ are, respectively, the state, input and output vectors and $w \in \mathbb{R}^n$ and $v \in \mathbb{R}^p$ are the process and the measurement noise, respectively, with covariance given by

$$E \left\{ \begin{bmatrix} w(t_1) \\ v(t_1) \end{bmatrix} \begin{bmatrix} w(t_2) \\ v(t_2) \end{bmatrix}^T \right\} = \begin{bmatrix} Q & S \\ S^T & R \end{bmatrix} \delta(t_2 - t_1).$$

The system matrices A , B , C and D are such that (A, C) is observable and $(A, [B, Q^{1/2}])$ is controllable. Assume that the following measurements are available:

- datasets $\{u(t_i), y(t_i)\}_{j, i \in [1, N], j \in [1, K]}$ of sampled input/output data (possibly associated with a non equidistant sequence of sampling instants) obtained from the true system are available. Specifically, data corresponding to the response of the helicopter to frequency sweeps, 3211 sequences and doublets have been collected.
- similarly, estimates $T(j\omega_i)$, $i \in [1, n_\omega]$ of the frequency response function of the helicopter, obtained from measured responses to frequency sweeps, are available, together with the corresponding values of the coherence function.

Then, the problem is to provide estimates of the state space matrices A , B , C and D (up to a similarity transformation) on the basis of the available data. Note that unlike most identification techniques, in this setting incorrelation between u and w, v is not required, so that this approach is viable also for systems operating under feedback.

3. ROTORCRAFT LINEAR MODEL IDENTIFICATION

The approach presented in this paper focus on the identification of linear models for flight dynamics, relying on the idea that low amplitude helicopter dynamics is well described by a linear model, assuming that airspeed, weight, centre of gravity, and altitude remain fixed. For this reason the three considered inputs sequences are applied to each axis in the same flight condition, while remaining close to the trim point.

More precisely, the approach to linear model identification for rotorcraft dynamics discussed in this paper follows the procedure depicted in Figure 1. As can be seen from the figure, and as mentioned in Section 2, the identification procedure uses input/output data collected in flight experiments in which three different types of input sequence are used, *i.e.*, frequency sweeps, 3211s and doublets. Frequency sweeps are the main source of information to identify the helicopter dynamics, while the doublets are used to cross-validate the identified models. At the end of the procedure data corresponding to the application of 3211 sequences is used to validate the results.

In the following subsections the main steps in the overall identification procedure are discussed.

3.1 Nonparametric frequency response function estimation

The commercial tool CIFER^[1] is used to compute nonparametric estimates of the frequency response functions of the helicopter, using the measured time responses to the frequency sweeps. As is well known, CIFER is a very reliable tool to carry out this task, as

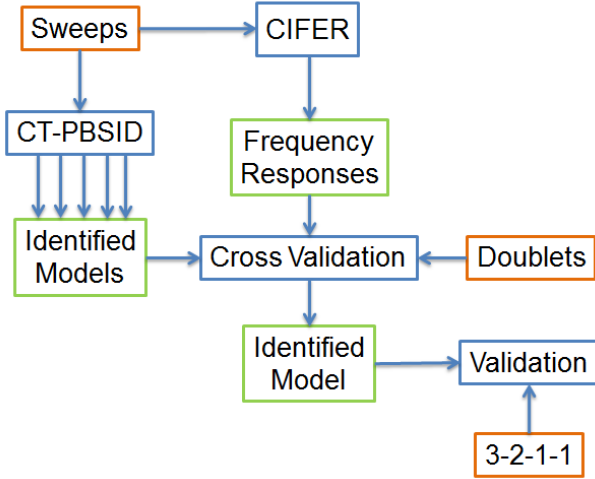


Figure 1: Scheme of the model identification procedure.

it has the desirable features of being able to extract frequency response function estimates from data also for multivariable systems, suitably tailored for the needs of rotorcraft identification problems. The output of this step is the set of estimates $T(j\omega_i)$, $i \in [1, n_\omega]$ of the frequency response function of the helicopter mentioned in Section 2.

3.2 Parametric black-box identification

The model identification of helicopter dynamics is performed using the Continuous-Time Predictor-Based Subspace Identification (CT-PBSID) black-box algorithm, which uses time-domain data to compute a black-box estimate of a linear state-space model in the form (1). A detailed presentation of CT-PBSID can be found in previous publications^[18]; in this paper only a concise description of the algorithm is provided:

- the time-domain data is converted to the Laguerre domain by means of the transformations

$$(2) \quad \begin{aligned} \tilde{u}(k) &= \int_0^\infty \ell_k(t) u(t) dt \\ \tilde{y}(k) &= \int_0^\infty \ell_k(t) y(t) dt \end{aligned}$$

where $\tilde{u}(k) \in \mathbb{R}^m$, $\tilde{y}(k) \in \mathbb{R}^p$ and $\ell_k(t)$ is the impulse response of the k -th Laguerre filter, defined as

$$(3) \quad \mathcal{L}_k(s) = \sqrt{2a} \frac{(s-a)^k}{(s+a)^{k+1}}.$$

- Using the transformed data, algebraic data equations are formed, to represent the input-output behaviour over a 'past' horizon p and a 'future' horizon f (in terms of the index k , now interpreted as a discrete-time index).
- From the data equations an estimate of the model order and of the state sequence of the system over the future horizon can be computed.

- Finally, the state space representation of the system in the discrete-time k can be estimated and the original continuous-time dynamics is recovered.

3.3 Cross validation

The CT-PBSID algorithm depends on some hyper-parameters, namely

- Laguerre pole a , *i.e.*, the position of the dominant pole of the Laguerre filters used to filter the input and output signals (see equation (3)). It should be greater than the dominant poles of the system and small enough to avoid numerical issues;
- past and future windows lengths, supposed equal ($f = p$).

Note that the choice of model order, *i.e.*, the supposed black-box model order, not directly linked to the expected physical differential equation order, must be also selected at this stage. The values of the hyper-parameters and the order of the model are chosen in the cross validation step, by minimizing

- the time-domain simulation error of the cross-validation data, *i.e.*, the difference between measured and simulated outputs;
- the frequency response function error, *i.e.*, a weighted combination of the magnitude and phase errors between the frequency response function estimates provided by CIFER and the frequency response functions of the identified models provided by CT-PBSID.

More precisely, the three hyper-parameters are selected using two time-domain metrics ($J_{TD_{max}}$ and $J_{TD_{median}}$) of the simulation error, *i.e.*, the difference between simulated and measured outputs, and four frequency-domain metrics ($J_{FD_{max_{DA}}}$, $J_{FD_{median_{DA}}}$, $J_{FD_{max_{CA}}}$, and $J_{FD_{median_{CA}}}$) of the frequency response error, *i.e.*, the difference between transfer functions and frequency responses.

The metric $J_{TD_{max}}$ is defined by adapting the root mean square fit error J_{RMS} ^[2] for the multi-output case taking the maximum, as follows

$$\begin{aligned} J_{TD_{max}} &= \max_{j \in \text{outputs}} J_{RMS}(j) \\ &= \max_{j \in \text{outputs}} \sqrt{\frac{1}{N} \sum_{i=1}^N (z_j(t_i) - y_j(t_i))^2}. \end{aligned}$$

It provides a useful overall measure of time-domain accuracy of the model. The simulation of unstable models, required by the computation of J_{RMS} , could be affected by numerical issues, and so a more robust cost function is preferred, *i.e.*,

$$J_{TD_{median}} = \text{median}_{j \in \text{outputs}} J_{RMS}(j)$$

$$= \text{median}_{j \in \text{outputs}} \sqrt{\frac{1}{N} \sum_{i=1}^N (z_j(t_i) - y_j(t_i))^2}.$$

where the median operator is involved. In case of single output the two indexes $J_{TD_{max}}$ and $J_{TD_{median}}$ coincide.

As for the frequency-domain, the cost function^[1]

$$J_{FD} = \frac{20}{n_\omega} \sum_{i=1}^{n_\omega} W_\gamma(\omega_i) \left[\left(|\hat{T}(\omega_i)| - |T(\omega_i)| \right)^2 + \frac{\pi}{180} \left(\angle \hat{T}(\omega_i) - \angle T(\omega_i) \right)^2 \right]$$

is used, where $\hat{T}(\omega_i)$ is the frequency response of the estimated model, $T(\omega_i)$ is the frequency response computed from the flight data, n is the number of frequencies ω_i selected in the bandwidth of interest, and $W_\gamma(\omega_i)$ is a weighting function defined as

$$W_\gamma(\omega) = \left(1.58 \left(1 - e^{-\gamma_{xy}^2(\omega)} \right) \right)^2$$

where $\gamma_{xy}(\omega)$ is the coherence function.

As already seen above for the time-domain root mean square fit error J_{RMS} , J_{FD} is adapted for the multi-output case taking the maximum, as follows

$$J_{FD_{max}} = \max_{i \in \text{inputs} \wedge j \in \text{outputs}} J_{FD}(j, i).$$

It provides a useful overall measure of frequency-domain accuracy of the model. A more robust cost function can be considered also in the frequency-domain, *i.e.*,

$$J_{FD_{median}} = \text{median}_{i \in \text{inputs} \wedge j \in \text{outputs}} J_{FD}(j, i).$$

Since the frequency-domain matching of the direct axis responses is the most valuable, the last two metrics are computed for the subset of all direct-axis (DA) responses, *i.e.*, q/δ_{lon} , p/δ_{lat} , r/δ_{ped} , N_y/δ_{ped} , and N_z/δ_{col} , and all the other responses, *i.e.*, cross-axis (CA) responses. The six metrics are usually different so the best compromise between them is searched.

3.4 Time-domain validation

The validation step provides the final check of the performance of the identified model, in the time-domain; indeed it is necessary to assess the capability of the identified models to describe data which have not been used neither for parameter estimation nor for cross-validation.

4. FLIGHT DATA RESULTS

In this section some results of the flight identification campaign for a light utility helicopter are presented, with specific reference to some flight test results in

terms of time-domain validation and Bode diagrams. More precisely, five speeds at the same flight condition (same weight, centre of gravity, and altitude) have been taken into account. As modern control theory allows to include in control law analysis and design the cross-axis effects if a MIMO model is provided, MIMO models have been identified considering as measured outputs the body angular rates, *i.e.*, p , q , r and the linear accelerations N_x , N_y , and N_z , and the pilot inputs (δ_{lon} , δ_{lat} , δ_{col} , and δ_{ped}).

4.1 Flight manoeuvre guidelines and constraints

In model identification experiments, the information content about the system under test is provided by the amplitude and phase relationships between the measured control inputs and outputs. The test input is one of the major factors that influence the identified model parameters accuracies. According to^[1], it should at least meet the following requirements:

- FCS off, since it tends to suppress the excitation signal and to correlate the input channels;
- all helicopter modes within the frequency range of interest must be properly excited;
- flight test duration must be long enough to provide sufficient low frequency information;
- aircraft response should stay within small perturbations limits from trim so that linearity assumptions are met;
- minor additional pilot inputs are allowed, *e.g.*, for maintaining the aircraft close to the trim condition.

Furthermore, usually the pilot maneuvers provide better signal-to-noise ratio since he/she is able to adapt the input magnitude according to the flight condition in every moment, the opposite of a predefined input signal. The magnitude of the input must be in the range of 2 ÷ 10% of control inputs. The resulting aircraft response should be around the trim of

- $\pm 3 \div 10\%$ deg, attitude;
- $\pm 3 \div 10\%$ deg/s, angular rates;
- $\pm 5 \div 10\%$ knots, air speed;
- $\pm 3 \div 10\%$ deg, sideslip angle.

In order to improve the frequency response computation, the input commands should start and end in trim condition.

Similar requirements and constraints apply for 3211s and doublets, though the excitation bandwidth of the signal is strictly tied to the time duration of each step^[2].

4.2 Time-domain comparison

The doublets are simple, fast, and cost effective maneuvers, and also they excite helicopter dynamics on all axes, even if not with the accuracy of 3211s and sweeps. For these reasons more than one repetition is usually asked to the pilot and those not used in the cross-validation step can be used in the validation step, as in the present case.

In Figure 2 a train of doublets is shown. The pilot is always in control of all axes to meet the constraints around trim discussed in the previous section.

Figure 3 shows the capability of the identified model to predict the helicopter response. Note that even if the model fails to match completely the amplitude of some of the peaks in the response of the rates, the overall dynamics is fully captured. Indeed looking at the simulation of the acceleration components, they appear to replicate the visible trend of the measured ones.

4.3 Frequency-domain comparison

The accuracy of the identified model can be verified in the frequency-domain by comparing its frequency response function to the non-parametric estimate obtained using CIPHER. As is well known the reliability of frequency response estimates is well quantified by the coherence function. In this study the coherence function plot is always omitted; the frequency responses are shown in the figures for all frequency points with coherence greater than 0.4. Information about the coherence is included by colouring samples of the on-parametric frequency response estimate as linear functions of the coherence, *i.e.*, black circles indicate coherence equal to 1, while light grey circle indicates coherence close to 0.4, as shown in 4.

The results are depicted in Figures 5-21. As can be seen from the figures, direct axis responses are well captured in the bandwidth of interest, but also several cross-axis responses are close to the flight data. Moreover the identified model is able to capture the natural frequency and the damping ratio of the dutch-roll mode even if the quality of the frequency response tends to decrease as shown in Figure 13.

4.4 Analysis of flight mechanics modes

Finally, in this section the variation of the flight mechanics modes, *e.g.*, dutch-roll and short period, as a function of the airspeed is shown. The considered speeds are such that $V_i > V_{i-1}$, with $i = 2, 3, 4, 5$. As shown in Figure 22 the damping of the dutch-roll mode tends to decrease for increasing airspeed, whilst the short-period mode shifts from an almost stable position to a slightly unstable one.

5. CONCLUDING REMARKS

A systematic approach to the identification of black-box models for rotorcraft dynamics combining time-domain and frequency-domain data using a continuous-time subspace identification algorithm has been described. With respect to existing methods, the proposed one does not include any iterative procedure, so that no initial guesses for the dynamics are needed, and can cope with data generated in closed-loop without introducing any bias. Experimental results obtained in the identification campaign for a light utility helicopter have been used to illustrate the time-domain and frequency-domain performance of the proposed method.

REFERENCES

- [1] M. Tischler and R. Remple. *Aircraft And Rotorcraft System Identification: Engineering Methods With Flight-test Examples*. AIAA, 2006.
- [2] R. Jategaonkar. *Flight Vehicle System Identification*. AIAA, 2006.
- [3] P. Hamel and J. Kaletka. Advances in rotorcraft system identification. *Progress in Aerospace Sciences*, 33(3-4):259–284, 1997.
- [4] P. Van Overschee and B. De Moor. *Subspace identification: theory, implementation, application*. Kluwer Academic Publishers, 1996.
- [5] M. Verhaegen and V. Verdult. *Filtering and System Identification: A Least Squares Approach*. Cambridge University Press, 2007.
- [6] M. Verhaegen and A. Varga. Some experience with the MOESP class of subspace model identification methods in identifying the BO105 helicopter. Technical Report TR R165-94, DLR, 1994.
- [7] S. Bittanti and M. Lovera. Identification of linear models for a hovering helicopter rotor. In *11th IFAC Symposium on system identification, Fukuoka, Japan*, 1997.
- [8] M. Lovera. Identification of MIMO state space models for helicopter dynamics. In *13th I-FAC Symposium on System Identification, Rotterdam, The Netherlands*, 2003.
- [9] P. Li and I. Postlethwaite. Subspace and bootstrap-based techniques for helicopter model identification. *Journal of the American Helicopter Society*, 56(1):012002, 2011.
- [10] M. Verhaegen. Identification of the deterministic part of MIMO state space models given in innovations form from input-output data. *Automatica*, 30(1):61–74, 1994.

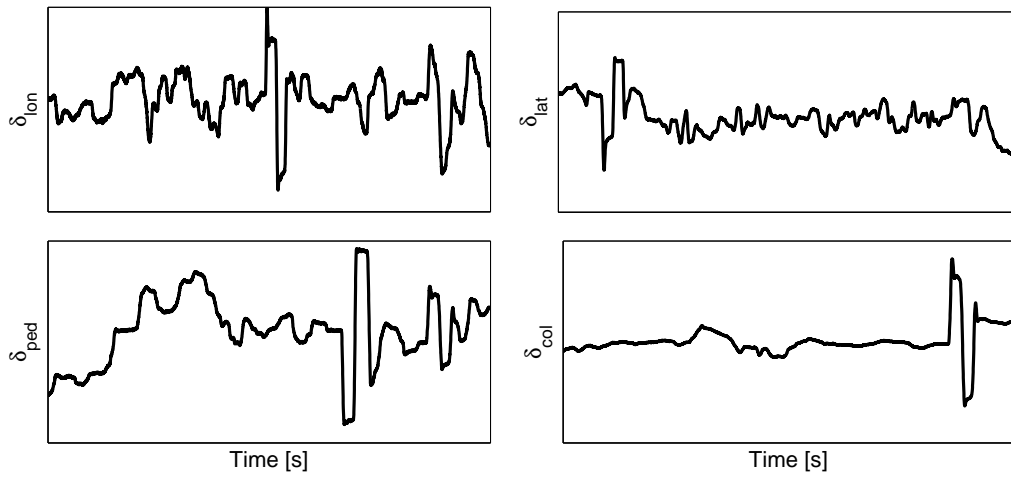


Figure 2: Validation data: doublet input signals applied on the control channels.

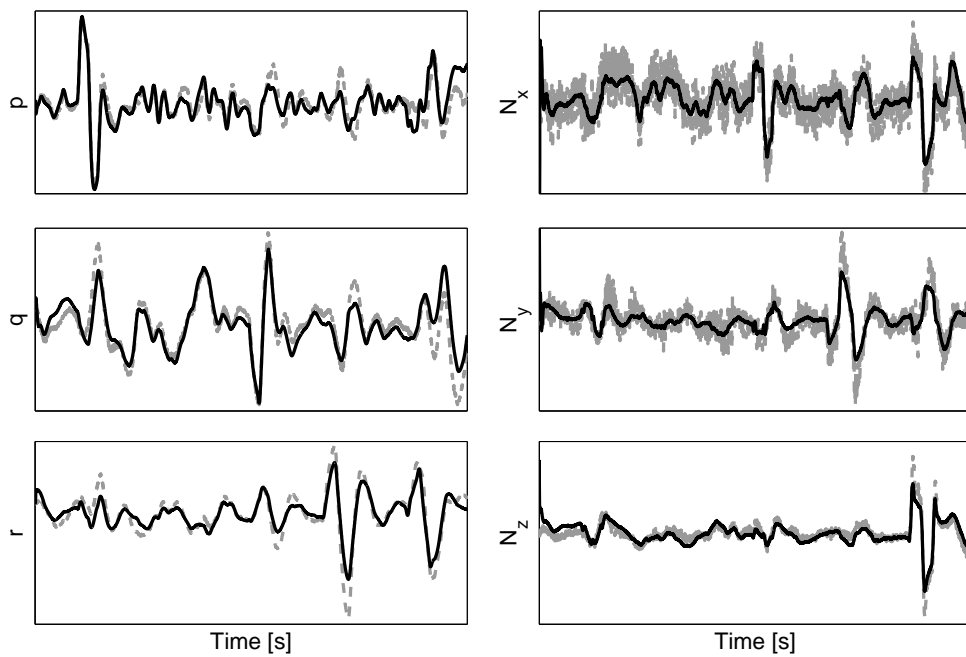


Figure 3: Validation data: responses of p , q , r , N_x , N_y , and N_z (measured: dashed line; simulated: solid line).

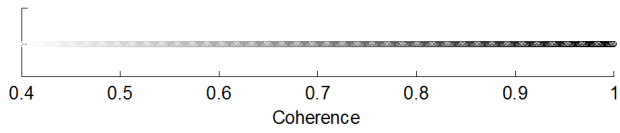


Figure 4: Legend of coherence function colormap.

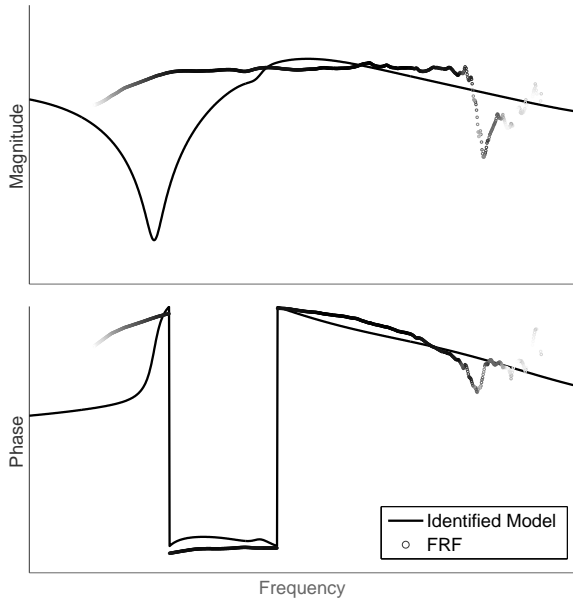


Figure 5: Bode plot of N_x/δ_{lon} .

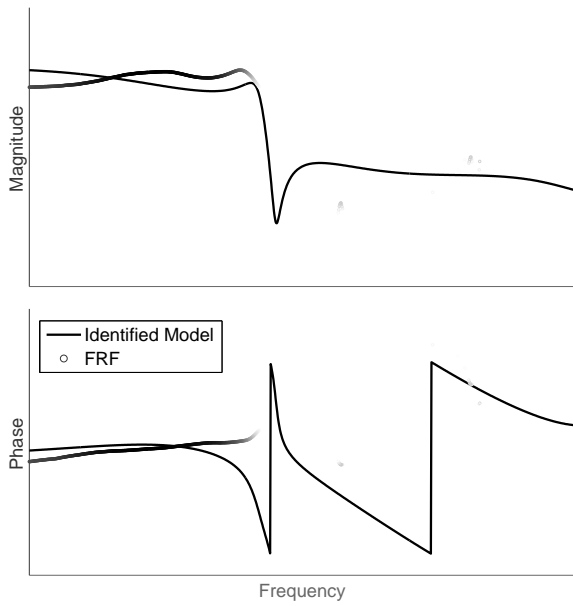


Figure 6: Bode plot of N_y/δ_{lon} .

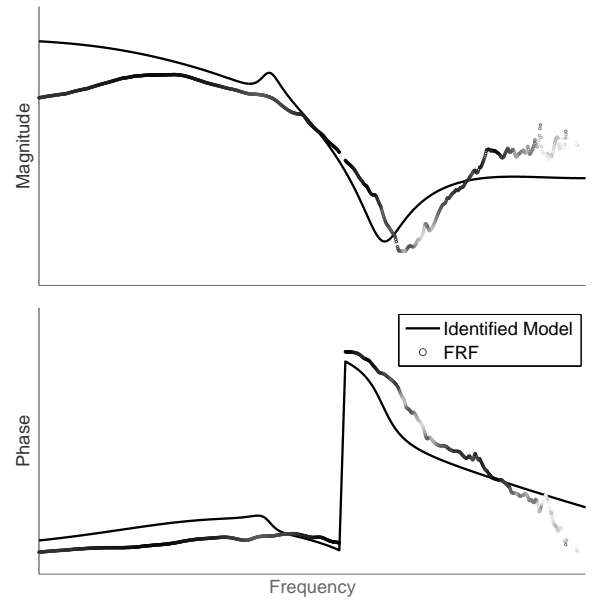


Figure 7: Bode plot of N_z/δ_{lon} .

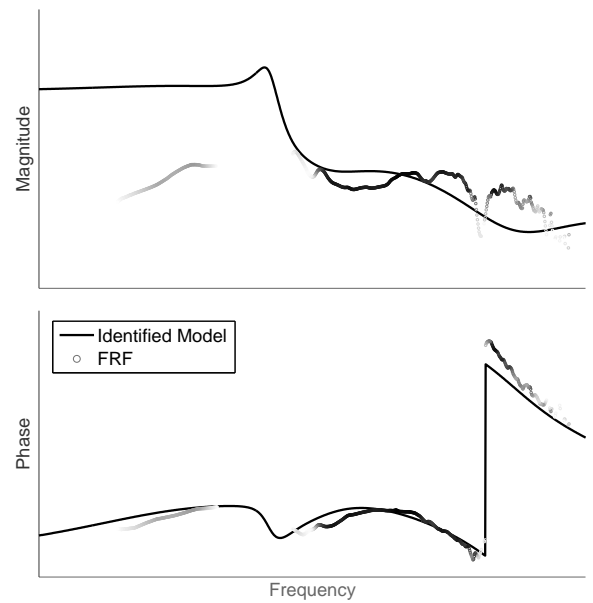


Figure 8: Bode plot of p/δ_{lon} .

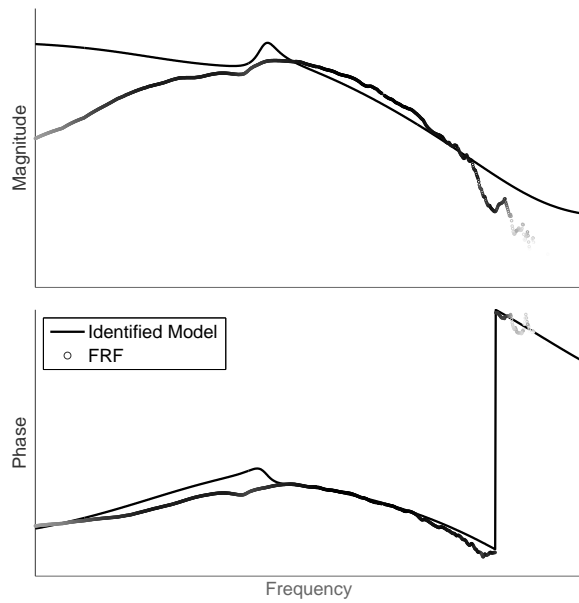


Figure 9: Bode plot of q/δ_{lon} .

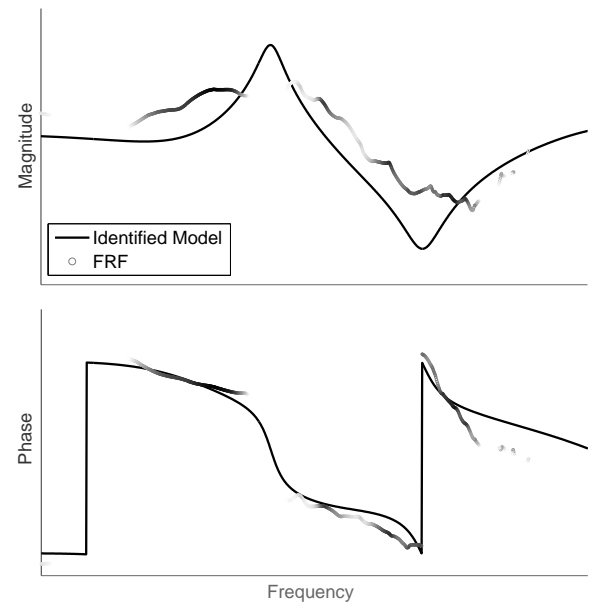


Figure 11: Bode plot of N_y/δ_{lat} .

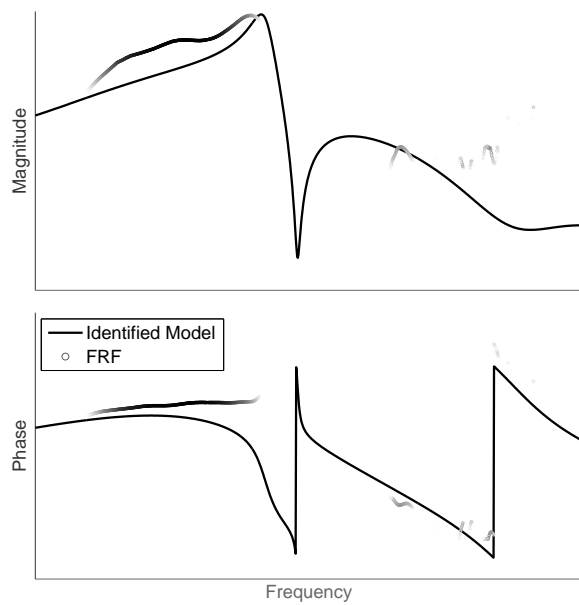


Figure 10: Bode plot of r/δ_{lon} .

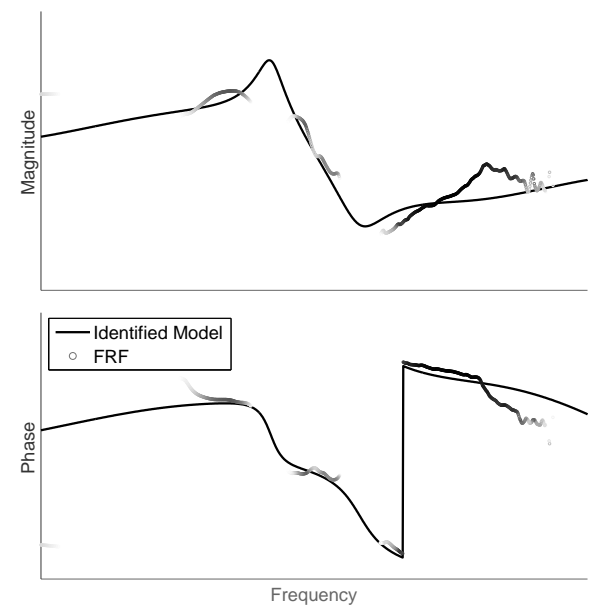


Figure 12: Bode plot of N_z/δ_{lat} .

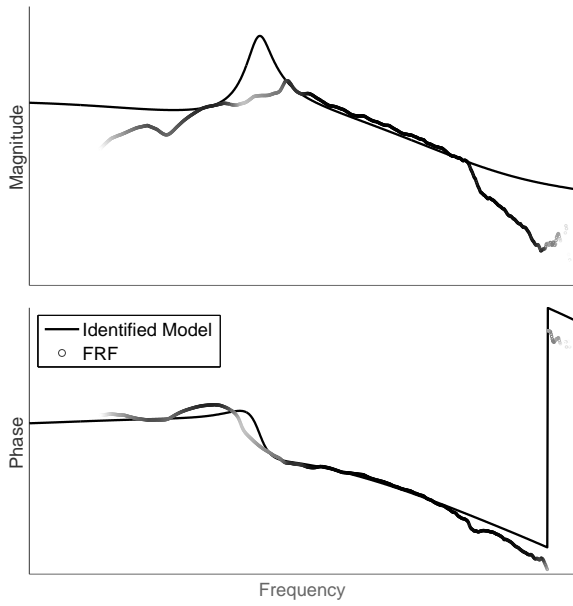


Figure 13: Bode plot of p/δ_{lat} .

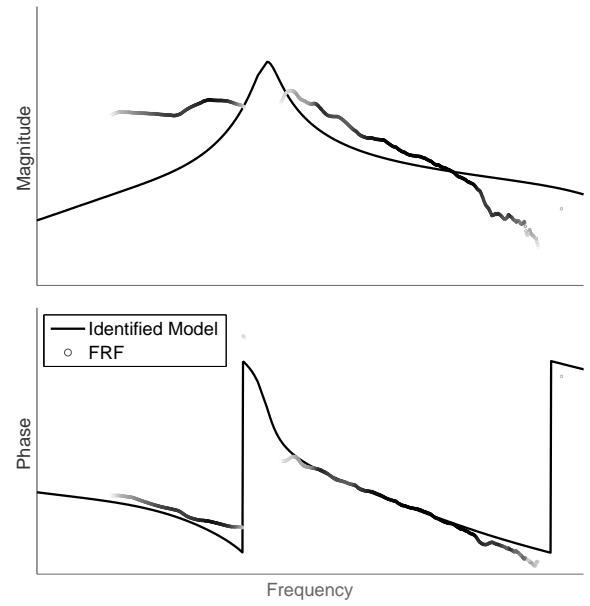


Figure 15: Bode plot of r/δ_{lat} .

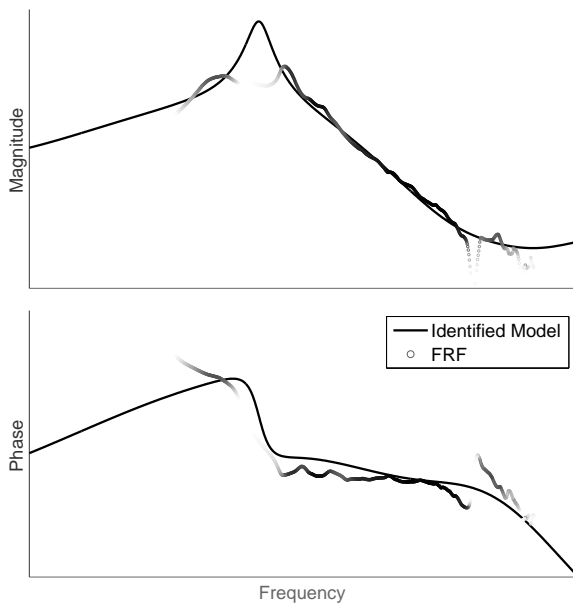


Figure 14: Bode plot of q/δ_{lat} .

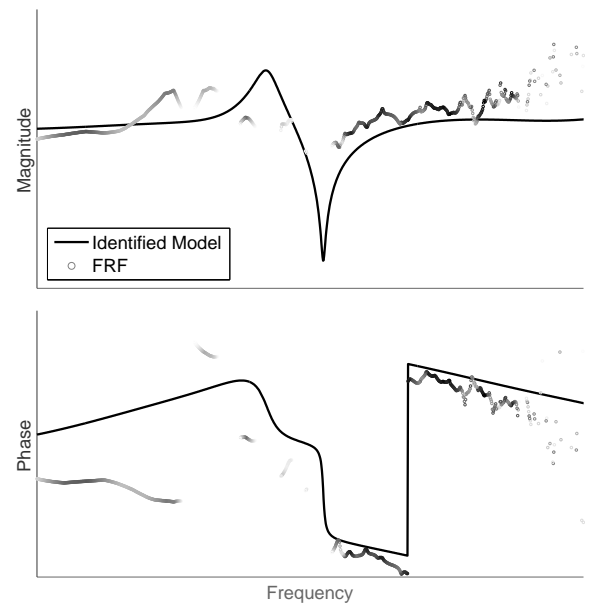


Figure 16: Bode plot of N_z/δ_{col} .

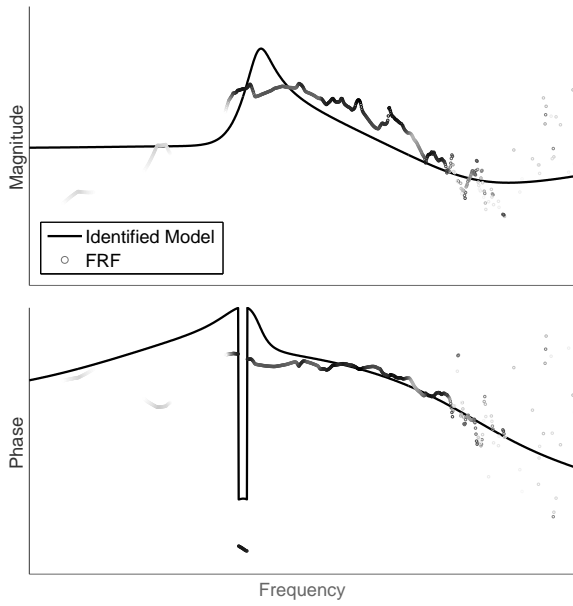


Figure 17: Bode plot of q/δ_{col} .

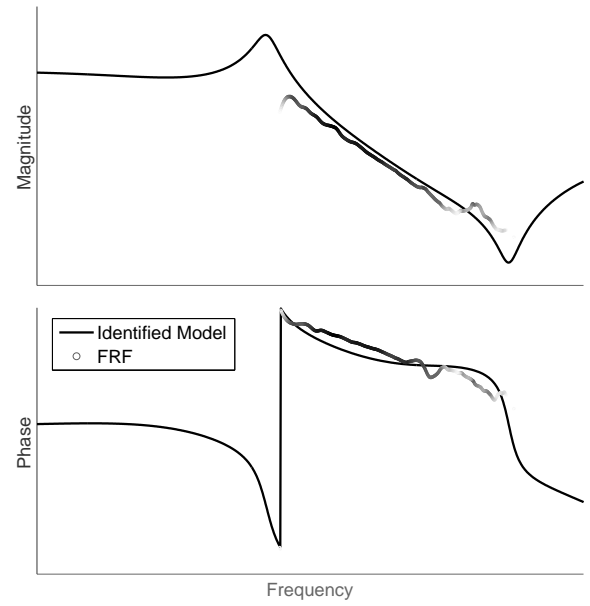


Figure 19: Bode plot of p/δ_{ped} .

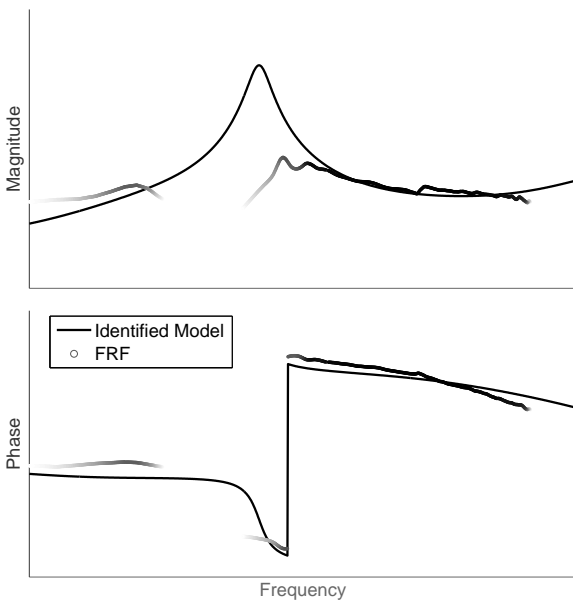


Figure 18: Bode plot of N_y/δ_{ped} .

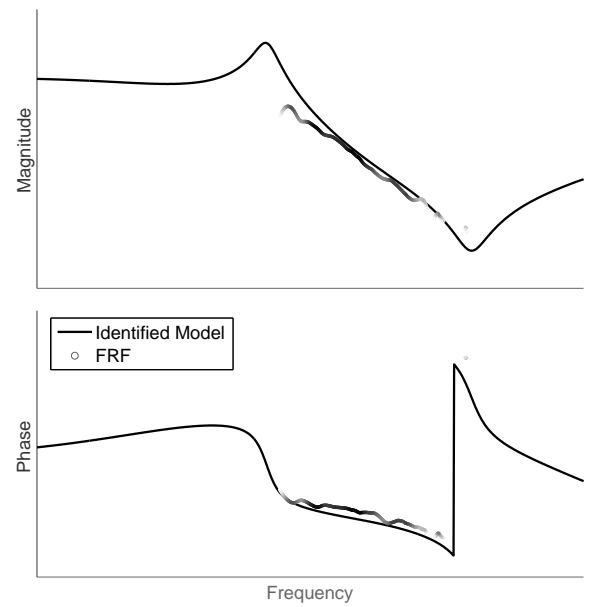


Figure 20: Bode plot of q/δ_{ped} .

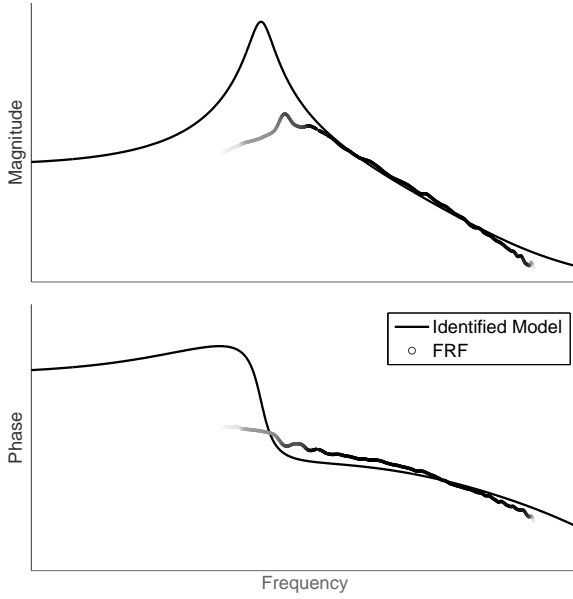


Figure 21: Bode plot of r/δ_{ped} .

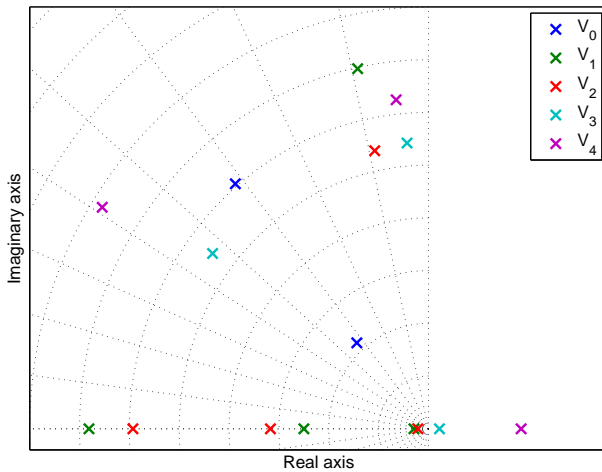


Figure 22: Eigenvalues of the flight mechanics modes for increasing speed.

- [11] S. Bittanti and M. Lovera. Bootstrap-based estimates of uncertainty in subspace identification methods. *Automatica*, 36(11):1605–1615, 2000.
- [12] A. Chiuso and G. Picci. Consistency analysis of certain closed-loop subspace identification methods. *Automatica*, 41(3):377–391, 2005.
- [13] B. Huang, S.X. Ding, and S.J. Qin. Closed-loop subspace identification: an orthogonal projection approach. *Journal of Process Control*, 15(1):53–66, 2005.
- [14] G. van der Veen, J. W. van Wingerden, Bergamasco M., Lovera M., and M. Verhaegen. Closed-loop subspace identification methods: an overview. *IET Control Theory and Applications*, 7(10):1339–1358, 2013.
- [15] J. W. van Wingerden. The asymptotic variance of the $PBSID_{opt}$ algorithm. In *16th IFAC Symposium on System Identification, Brussels, Belgium*, 2012.
- [16] M. Bergamasco, M. Lovera, and Y. Ohta. Bootstrap-based model uncertainty assessment in continuous-time subspace model identification. In *52th IEEE Conference on Decision and Control (CDC)*, pages 5840 – 5845, Florence, Italy, 2013.
- [17] M. Bergamasco and M. Lovera. Continuous-time predictor-based subspace identification for helicopter dynamics. In *37th European Rotorcraft Forum, Gallarate, Italy*, 2011.
- [18] M. Bergamasco and M. Lovera. Continuous-time predictor-based subspace identification using Laguerre filters. *IET Control Theory and Applications*, 5(7):856–867, 5 2011.
- [19] Y. Ohta. Realization of input-output maps using generalized orthonormal basis functions. *Systems & Control Letters*, 22(6):437–444, 2005.
- [20] M. Bergamasco, A. Ragazzi, and M. Lovera. Rotorcraft system identification: a time/frequency domain approach. In *19th IFAC World Congress, Cape Town, South Africa*, 2014.
- [21] M. Bergamasco and M. Lovera. Identification of linear models for the dynamics of a hovering quadrotor. *IEEE Transactions on Control Systems Technology*, 22(5):1696–1707, 2014.